Journal of Al-Nahrain University Vol.12 (1), March, 2009, pp.14-23 Science

THEORETICAL STUDY OF CONCERTED DIELS-ALDER REACTIONS BETWEEN DIMETHYL 1,2,4,5-TETRAZINE-3,6-DICARBOXYLATE AND DIENOPHILES

Jewad Kadhum Shneine, Shaima Mohamad Ali Mahmood and Mehdi Salih Shihab
Al-Nahrain University, College of Science, Department of Chemistry, Al-Jadrya, Baghdad-Iraq.

Abstract

Computational study at different levels of quantum calculations (AM1, PM3 and ab initio (HF/3-21G)) where preformed on the inverse-demand synchronous concerted Diels-Alder reactions between dimethyl 1,2,4,5-tetrazine-3,6-dicarboxylate as a diene and a variety of dienophiles (ethylene, cyclopentadiene, 1-hexene, cyclohexene). All the molecular structures (reactants, transition states, intermediates and adducts) were optimized by AM1 method. The calculated energies and volumes showed that the cycloaddition systems followed a mechanism by formation an intermediate and proceed to eject N_2 molecule and ended by 1,2-hydrogen shift adduct. The prediction of the reaction energies of modeling of the cycloaddition reactions under-study by semiempirical AM1 method showed a good agreement with the experimental data comparing with PM3 and HF/3-21G. whereas, the prediction of activation energies by (AM1, PM3 and ab initio (HF/3-21G)) showed overestimated values comparing with experimental data.

Introduction

The Diels-Alder reaction is one of the most useful system for organic synthesis to obtain six-membered heterocycles and has attracted much interest both experimentally[1,2] and theoretically[3,4]. The semi-empirical levels were performed on model intra- and inter-molecular Diels-Alder systems, which showed good agreements in the modeling the cycloaddition reactions[5].

In particular, the well defined participation of 1,2,4,5-tetrazines in [4+2] cycloadditions serve as useful intermediates for the preparation of a variety of ring systems natural products [6,7]. The methodology is based on an inverse electron demand Diels-Alder reaction of an electron-deficient 1,2,4,5-tetrazine as dienes with an electron-rich dienophile to form a 1,2-diazine and followed by a 1,3-hydrogen shift[8].

In this paper, we report theoretical study of mechanism on four inverse-demand Diels-Alder reactions using the inexpensive semi-empirical method at the restricted Hartree–Fock (RHF) formalism. The general mechanism reaction (Scheme1) begins with a [4+2]-cycloaddition of dimethyl 1,2,4,5-tetrazine-3,6-dicarboxilate as diene to different dienophiles (ethylene, cyclopentadiene, 1-hexene, cyclohexene). In both suggesting cases of path way A and path way B mechanisms, the addition is followed by elimination of the nitrogen molecule from the resulting intermediate, leading to the formation of (substituted) dihydropyridazine.

Computational methods

Present systems in this work avoided to optimize at the ab initio level because it is exceedingly expensive. However, semi-empirical methods have progressed over the past few years to a surprising level of accuracy and reliability, considering the limitations of the underlying approximations[9]. Even simple calculations at moderate levels of theory such as semiempirical procedures give useful information on the molecular mechanism for different chemical reactions. AM1 Hamiltonian[10] as implemented in the program package HyperChem version 7.1 [Hypercube Inc. Gainsville FL.]. Initial molecular using geometries of all structures were optimized with the AM1 semi-empirical method without constraint in the final run of the calculation. Vibrational frequencies were then computed to characterize each stationary structure as a

minimum or transition states (TS), via the number of imaginary frequencies (zero for minima and one for saddle points, respectively). The total energies (E_{total}) were estimated from AM1 and PM3[11a] and single point calculations on the HF/3-21G models[11b] at optimized geometries (with AM1) in order to minimize computational cost. To estimate activation energies the conventional transition state theory has been accepted and that based on the adiabatic potential energy surfaces rather than on free energy surfaces. Initial TSs for the rearrangements were obtained by constrained optimizations in which the corresponding forming or breaking bond was systematically varied while all other geometrical variables were fully optimized. These guess structures were subsequently refined to TS by full optimizations. All results reported in this work refer to such completely verified reactant–TS–product triples. Unless noted, AM1 energies (zero point energies constraining geometries were not included) are used for discussion throughout the text. Finally, all calculations in this investigation, were performed in the gas phase.

Program package HyperChem version 7.1 has option to use the quantitative structure-activity relationships (QSAR) which are attempts to correlate molecular structure[12], using the atomic radii of Gavezotti[13]. This calculation is used to calculate the Van der Waals-surface-bounded molecular volume (V_i, Å^3) for some present molecular structures and by multiplying (V_i) with Avogadro's number (N_A, mol^{-1}) to get the volume occupied by a molecule which is called van der Waals volume (V_w cm^{3}ml^{-1}) [14].

All the reactions consider in this study are assumed to follow essentially a synchronous and concerted mechanism because the symmetry of diene and dienophiles (slightly difference in molecular orbital coefficients for 1-hexene).

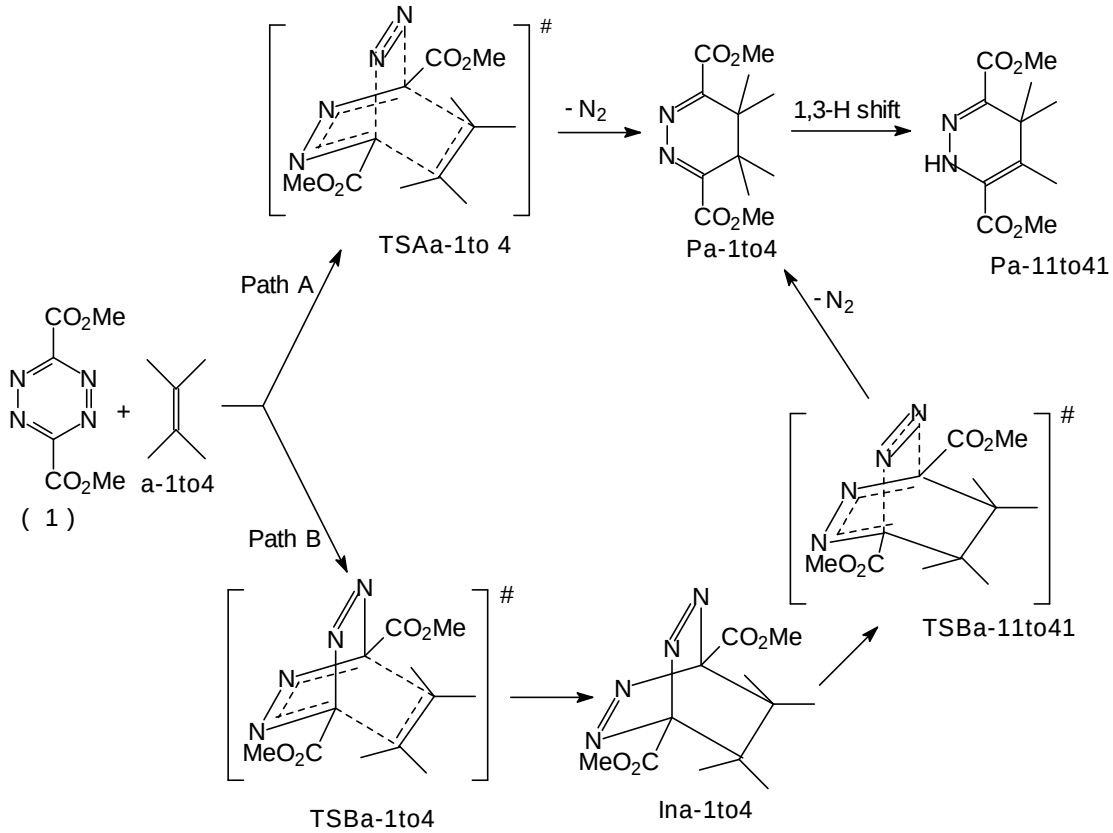

a-1: ethylene; a-2: cyclopentadiene; a-3: 1-hexene; a-4: cyclohexene

Scheme (1) : Four inverse-demand Diels-Alder reactions of dimethyl 1,2,4,5-tetrazine-3,6-dicarboxilate as diene with different dienophiles (ethylene, cyclopentadiene, 1-hexene, cyclohexene) and the Diels-Alder reactions proceed with path way A and path way B mechanisms.

Results and discussion

We have studied firstly the structures of ethylene (**a-1**)**,** cyclopentadiene (**a-2**)**,** 1-hexene (**a-3**)**,** cyclohexene (**a-4**) as dienophiles and dimethyl 1,2,4,5-tetrazine-3,6-dicarboxilate(**1**) as a diene, as shown in Fig.(1). Planar conformations have been located for (**a-1**)**,** (**a-2**) and (**1**) except (**a-3**) and (**a-4**).

Generally, mechanism route of Diels-Alder reaction proceeds by approach reactants (diene [C_3,C_6] and dienophile [C_1,C_2]) with each other by a way that makes the planes of each reactant are canted for easy overlap of π-electrons to form new bonds [15].

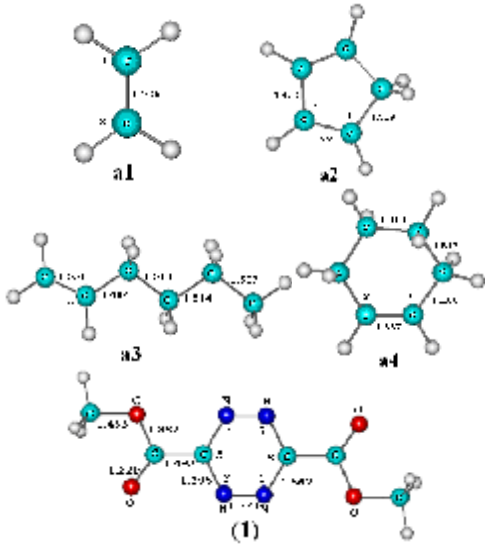

Fig.(1): AM1 optimized geometries of ethylene (a-1), cyclopentadiene (a-2), 1-hexene (a-3), cyclohexene (a-4) and dimethyl 1,2,4,5-tetrazine-3,6-dicarboxilate (1). Bond lengths are given in Å.

The calculated total energies (E_{total}) of reactants and products, and the frontier orbital energies are gathered in Table 1. A normal Diels–Alder reaction involves an electron-rich diene or analogue and an electron-poor dienophile, but in the systems under study, the calculated frontier orbital energies (Table 1) for HOMO (highest occupied molecular orbital)-LUMO (unoccupied molecular orbital) pair of each reactants (energy gap (*DE*1, *DE*2)) show that both the cycloaddition of Diels–Alder reaction between (**1**) and **(a-1 to a-4)** exhibit inverse electron demand. The low values of *DE*2 in Table (1) are confirming this fact. This means that if (1) behaves as a diene reagent in Diels–Alder cycloaddition, the reaction will be favored when the dienophile is electron-rich. And also The AM1 calculated polarization of the relevant frontier orbitals of dimethyl 1,2,4,5-tetrazine-3,6-dicarboxilate shows a higher contour value at C_3 and at C_6 in LUMO orbital than that in HOMO orbital (see Figure 2). This polarization explains the inverse Diels-Alder reaction of this compound **(1)**.

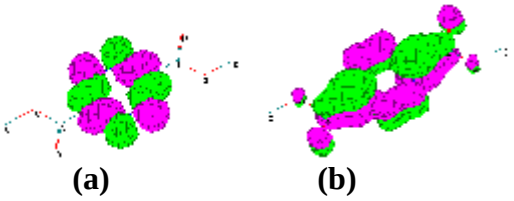

Fig.(2): AM1 calculated polarization of HOMO (a) and LUMO (b) orbitals of dimethyl 1,2,4,5-tetrazine-3,6-dicarboxilate.

Table (1)
Calculated the total energies (E_{total}) of reactants and products. Frontier orbital energies of the HOMO and LUMO of the reactants (with AM1 method).

Compounds	E_{total}	HOMO	LUMO	$\Delta E1$[a]/eV	$\Delta E2$[b]/eV
1	-68199.8	-11.4256	-2.5164		
a-1	-7157.3	-10.5516	1.4378	12.68	8.04
a-2	-16637.7	-9.0786	0.4816	11.91	6.56
a-3	-21534.6	-9.9254	1.3686	12.79	7.41
a-4	-20901.5	-9.4906	1.3273	17.75	6.97
Ina-1(path B)	-75377.1				
Ina-2(path B)	-84852.6				
Ina-3(path B)	-89745.5				
Ina-4(path B)	-89107.4				
Pa-1	-65874.1				
Pa-2	-75331.8				
Pa-3	-80244.0				
Pa-4	-79605.1				
Pa-11	-65876.1				
Pa-21	-75350.3				
Pa-31	-80245.6				
Pa-41	-79610.4				
N_2	-9550.3				

[a]*DE1*= $HOMO_{diene}$-$LUMO_{dienophile}$. [b]*DE2*= $LUMO_{diene}$-$HOMO_{dienophole}$

According to Scheme 1, adducts **(Pa-1** to **Pa-4)**could be obtained from **(1)** with different dienophiles (a-1 to a-4) via two different possible mechanisms. The mechanism (A) involves one step synchronous cycloaddition Diels–Alder reaction or synchronous

cycloaddition mechanism (B) proceeds through intermediate (Ina-1when (a-1) is dienophile). A question can be posed; does the reaction in Scheme 1 proceed via mechanism of path (A) or path (B)?. We attempt to answer this question by a theoretical analysis using a semi-empirical approach.

1. Cycloaddition via path (A)

In principle, the carbon-carbon double bonds of dienophiles (**a-1** to **a-4**) can add to diene (**1**) in a proper conformation for the cycloaddition reaction. Simultaneously, there are C-C bonds formation and C-N breaking (this step is determining of the reaction rate). In other words, the addition of alkene and elimination of N_2 molecules take place in the same time (see scheme 1). Fig.(3) and Table (2) are depicted the important optimized geometries parameters of the transition state (TS) and values for path A between diene (**1**) and dienophiles (**a-1** to **a-**4). The synchronous saddle points are characterized as true transition states, possessing one imaginary frequency, by frequency calculations in all cases.

In Fig. (3), we show four transition states for the cycloaddition reactions (**TSAa-1 to TSAa-4**) from different approaching dienophiles with breaking C-N bonds to leave as N_2, synchronously.

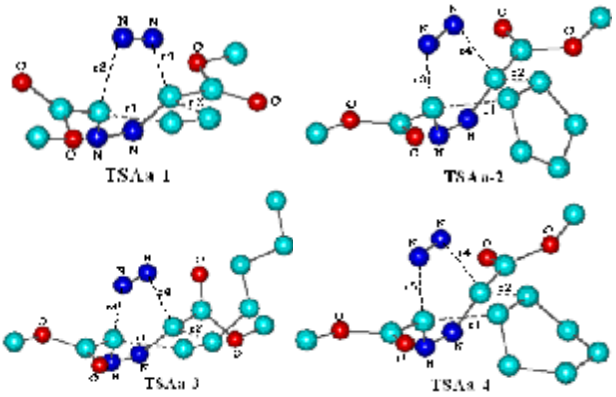

Fig. (3): Optimized geometries for four transition states of path A with AM1 method. Hydrogen bonds omitted for clarity.

The distances *r***1** and *r***2** in Tables (2) refers to the two single bonds being formed synchronously. The parameter *a*, defined as $a = (r1 - r2)/(r1 + r2)$, represents the degree of asynchronicity]16]. The greater the value of *a*, the less the transition state is synchronous. Because the Diels–Alder reaction needs a good synchronization, the *a* value is then an important index. The synchronicity of these transition states (**TSAa-1 to TSAa-4**) are very high (*a* is a very weak value).

Table (2)

Parameters for different transition states of Diels–Alder reaction between (1) and a-1 to a-4, computed with the AM1 method.

T.S.	E_{total} [b]	E_a [b]	r_1/Å	r_2/Å	r_3/Å	r_4/Å	α[a]
TSAa-1(path A)	-75288.5	67.3	2.111	2.090	1.704	2.065	0.0053
TSAa-2(path A)	-84765.1	44.6	2.185	2.049	1.723	2.056	0.0324
TSAa-3(path A)	-89656.5	59.9	2.227	2.009	1.673	2.106	0.0512
TSAa-4(path A)	-89021.4	54.2	2.116	2.109	1.739	2.044	0.0023
TSBa-1(path B)	-75338.7	18.4	2.119	2.096			0.0054
TSBa-2(path B)	-84814.9	22.6	2.191	2.058			0.0031
TSBa-3(path B)	-89709.9	24.7	2.235	2.014			0.0052
TSBa-4(path B)	-89071.5	29.8	2.116	2.126			0.0035
TSBa-11(path B)	-75357.1	20.0			1.710	2.074	
TSBa-21(path B)	-84833.3	19.3			1.730	2.060	
TSBa-31(path B)	-89724.6	20.9			1.675	2.112	
TSBa-41(path B)	-89087.6	19.8			1.745	2.049	

[a] ***α : degree of asynchronicity defined as (r2 - r1)/(r2 + r1).***

[b] ***total energy and energy of activation in/kcal mol^{-1} [$E_a = (E_{total})_{TS} - S_i\{(E_{total})_i\}_{reagents}$].***

2. Cycloaddition via path (B)

In principle, the C=C bond of dienophiles (**a-1** to **a-4**) can add to diene (**1**) in a proper conformation for the cycloaddition reaction. There are C-C bonds formation between a diene and a dienophile (this step is determining of the reaction rate). But the elimination of N_2 molecule takes place in second step (see Scheme (1). Fig. (4) and Table (2) are depicted the important optimized geometries parameters of the transition state and values for path B between diene (**1**) and dienophiles (**a-1** to **a-4**). The synchronous saddle points are characterized as true transition states, possessing one imaginary frequency, by frequency calculations in all cases. In Fig. (4), we show four transition states for the cycloaddition reactions (**TSBa-1 to TSBa-4**) from different approaching dienophiles that takes place synchronously. The distances ***r*1** and ***r*2** in Tables (2) refers to the two single bonds being formed synchronously. The synchronicity of these transition states (**TSBa-1 to TSBa-4**) are very high (α is a very weak value).

If we compare the activation energies of path A and path B by taking a sight to Table (2) , its clear that the activation energies of transitions states (**TSBa-1 to TSBa-4**) are less by more than two times than the activation energies of transitions states (**TSAa-1 to TSAa-4**) and also the all values of van der Waals volumes(V_w) of (**TSBa-1 to TSBa-4**) are less than (**TSAa-1 to TSAa-4**) (see Table (3)). The calculated activation volumes ($D\,V^{\#}$) for path A and path B in Table 3 were shown the transitions states (**TSBa-1 to TSBa-4**) of path B more compact than transitions states (**TSAa-1 to TSAa-4**). The experimental data confirmed our anticipation for path B [17]. Therefore, the path B is favor to proceed for this kind of Diels-Alder reactions. Fig.(5) is shown energy profile for the cycloaddition reaction of **(a-1)** and **(1)** to depict the comparison between the stability of transition state of path A and path B.

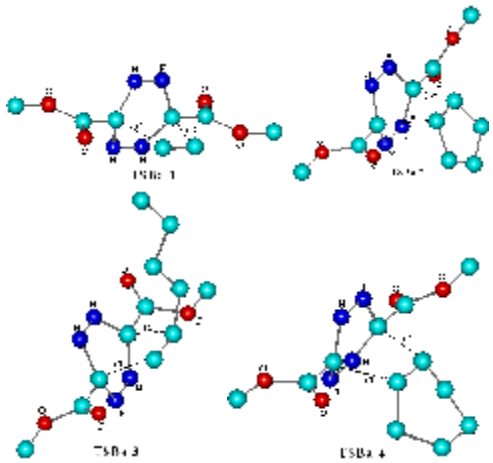

Fig. (4): Optimized geometries for four transition states of path B with AM1 method. Hydrogen bonds omitted for clarity.

Table (3)
The van der Waals volumes (V_w) of reagent and transition states of path A and path B and calculated volume of activation ($D V^{\#}$).

molecules	V_w[a], $cm^3 mol^{-1}$	$\Delta V^{\#}$[b], $cm^3 mol^{-1}$
1	153.5	
a-1	40.9	
a-2	76.4	
a-3	108.6	
a-4	96.9	
TSAa-1(path A)	189.3	-5.1
TSAa-2(path A)	224.7	-3.2
TSAa-3(path A)	256.6	-6.0
TSAa-4(path A)	245.4	-5.0
TSBa-1(path B)	186.0	-8.4
TSBa-2(path B)	221.7	-6.2
TSBa-3(path B)	253.3	-8.8
TSBa-4(path B)	242.1	-8.3

[a] V_w [by (QSAR)].
[b] $\Delta V^{\#}=(V_w)_{TS}-\Sigma_i\{(V_w)_i\}_{reagents}$

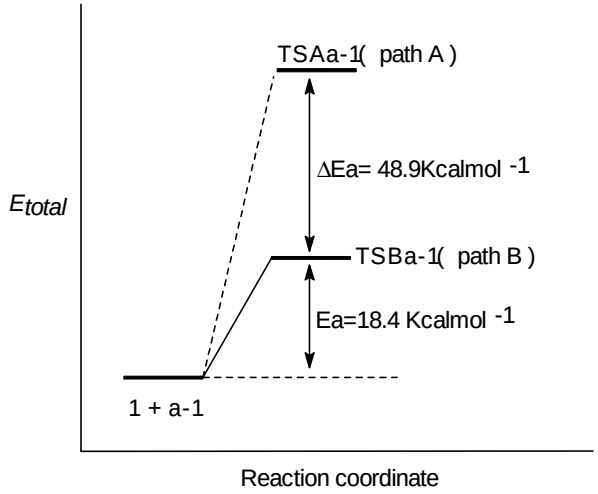

Fig. (5) : Energy profile for the cycloaddition reaction of ethylene and dimethyl 1,2,4,5-tetrazine-3,6-dicarboxilate to depict the comparison between the stability of transition state of path A and path B.

3. Cycloaddition of path (B) by AM1 and other methods of quantum calculation

We fixed that the process of path B proceeds for the systems under study, and the profile energy of path B (data from Tables (1 and 2)) could be depicted in Fig. (6) which shows two steps of cycloaddition reaction of 1-hexene and dimethyl 1, 2, 4, 5-tetrazine-3, 6-dicarboxilate, as example. All other dienophiles (cyclopentadiene, ethylene and cyclohexene) with dimethyl 1, 2, 4, 5-tetrazine-3, 6-dicarboxilate fellow the same way of the energy profile. All geometries of structures of all steps of path B were optimized starting from the reactants to the finial adducts (see Figs. 1, 4, 7-10). In Fig. (7), it's shown the optimized geometries for four intermediates **Ina-1** to **Ina-4** of concerted cycloaddition reaction of second step of path B using AM1 method. These intermediates are relatively stable (exothermic step) comparing with the reactants (see the values of $DE_{rn}1$ in Table (4)). In Fig.(8), it's shown optimized geometries for four transition states **TSBa-11** to **TSBa-21** of path B (this step is not determining of the reaction rate) using AM1 method (The synchronous saddle points are characterized as true transition states, possessing one imaginary frequency, by frequency calculations in all cases). Since these transition states including elimination of nitrogen molecule, therefore, the values of activation energies (Ea2) have approximately the same values (see Table (4)). And also there is a lower synchronous in the ejection step of nitrogen molecule in this step, because the difference in values of r3 and r4 (see Table (2)).

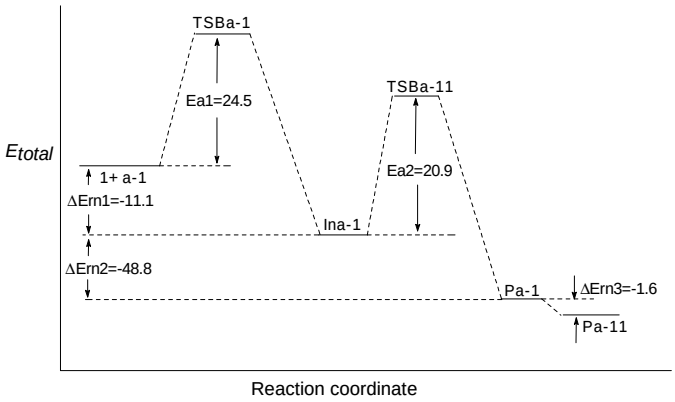

Fig. (6) : Energy profile in kcal mol^{-1} for the cycloaddition reaction of 1-hexene and dimethyl 1,2,4,5-tetrazine-3,6-dicarboxilate for path B.(data of Tables 1,2, AM1 method).

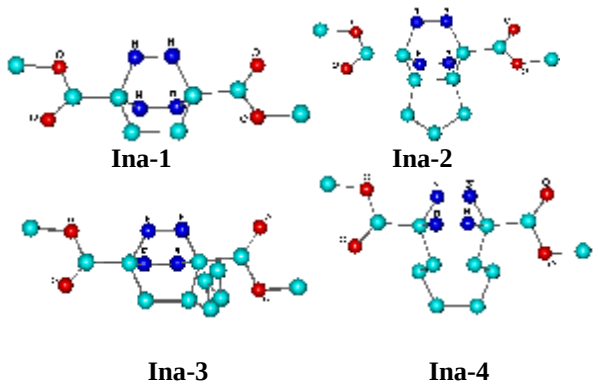

Fig.(7) : Optimized geometries for four intermediates of path B with AM1 method. Hydrogen bonds omitted for clarity.

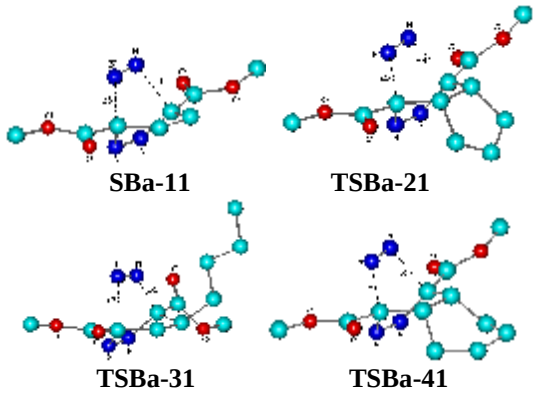

Fig. (8) : Optimized geometries for four transition states of second step of path B with AM1 method. Hydrogen bonds omitted for clarity.

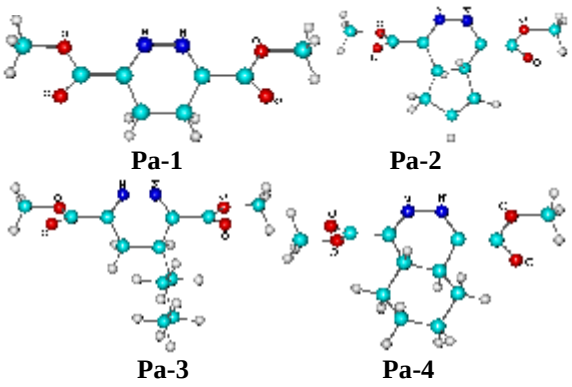

Fig. (9) : Optimized geometries for four adducts with AM1 method.

Fig. (9) is shown the optimized geometries for four adducts **Pa-1** to **Pa-4** (1,2-diazines) with AM1 method. These adducts (**Pa-1** to **Pa-4**) have high stability (exothermic step) than reactants (see Fig (6)), but 1,2-diazines are followed by a 1,3-hydrogen shift [8] to obtained the final adducts **Pa-11** to **Pa-41** as show in Fig. (10). The relative stability of final adducts to 1,2-diazines are depicted in Table (4).

We want to extend our quantum calculations with other levels of calculation to make comparison for how much the selected method of calculation (AM1) can correlated with the others (quantum calculations and experimental data[17,18] from standpoints of energies.

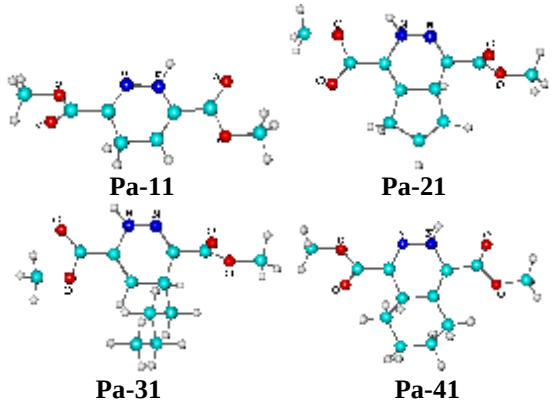

Fig. (10) : Optimized geometries for four final adducts with AM1 method.

Therefore, all the total energy of structures in path B were recalculated by using PM3 level (see Table(5)) and repeating that calculations by using single point calculations on the HF/3-21G level on optimized geometries obtained at semiempirical AM1 level (see Table(6)). In Table 4 we calculated the activation energies and reaction energies of different steps of path B by using AM1 (the same way, as shown in Fig.(6)). The calculations showed that the present cycloaddition systems have high activation energy and high exothermicity. Fig.(10) is shown comparison of experimental data of enthalpy of reaction of the concerted Diels-Alder reactions of ethylene**,** cyclopentadiene**,** 1-hexene and cyclohexene with dimethyl 1,2,4,5-tetrazine-3,6-dicarboxilate with different levels of quantum calculations. The experimental data was obtained from literatures to show reliability of use the low cost of quantum calculations to apply for the concerned Diels-Alder reactions. In Fig.(10), it's clear that the AM1 level shows a good correlation with the experimental data than with the other levels (PM3, HF/3-21G), this correlation was confirmed by Narahari el et [19] and showed that low cost semiempirical calculations (AM1,PM3) were better performance in modeling of the Diels-Alder reactions in large systems with the ab initio and density functional theory (DFT) calculations are prohibitively expensive. From another side, unfortunately, we found that the values of calculated activation energy of the determining step of the rate of path B between diene **(1)** and

1-hexene by using AM1, PM3 and HF/3-21G are 24.5, 37.9, 23.6 kcal mol^{-1}, respectively (see Tables (3-5)). And these values are overestimated comparing with the experimental value of the activation energy which is 8.6 kcal mol^{-1} (in Dioxane) for the same reaction [17].

Table (4)

Calculated total energy in kcal mol^{-1} of reactants, transition states and products of path B, computed with the AM1 method. Enthalpy of reaction (DE_{rn}) and activation energy(Ea) as depicted in Fig. (6).

Compounds	E_{total}	$\Delta E_{rn}1$	$\Delta E_{rn}2$	ΔE_{rn}(total)[b]	$Ea1$	$Ea2$	Experimental Data (ΔE_{rn})[c]
1	-68199.8						
a-1	-7157.3			-69.3			-69.8
a-2	-16637.7			-58.6			-60.3
a-3	-21534.6			-61.5			-67.9
a-4	-20901.5			-59.4			-65.1
Ina-1	-75377.1	-20.0					
Ina-2	-84852.6	-15.1					
Ina-3	-89745.5	-11.1					
Ina-4	-89107.4	-6.1					
Pa-1	-65874.1		-47.3				
Pa-2	-75331.8		-29.5				
Pa-3	-80244.0		-48.8				
Pa-4	-79605.1		-48.1				
Pa-11	-65876.1		-2.0[a]				
Pa-21	-75350.3		-14.0[a]				
Pa-31	-80245.6		-1.6[a]				
Pa-41	-79610.4		-5.2[a]				
N_2	-9550.3						
TSBa-1	-75338.7				18.4		
TSBa-2	-84814.9				22.6		
TSBa-3	-89709.9				24.5		
TSBa-4	-89071.5				29.8		
TSBa-11	-75357.1					20.0	
TSBa-21	-84833.3					19.3	
TSBa-31	-89724.6					20.9	
TSBa-41	-89087.6					19.8	

[a] DE_{rn}**3 (see Fig. 6).** [b] DE_{rn}**(total) =** DE_{rn}**1 +** DE_{rn}**2 +** DE_{rn}**3.** [c] **see ref. [17,18], enthalpies of reaction of experimental data in kcal mol^{-1}**

Table (5)

Calculated total energy in kcal mol^{-1} of reactants, transition states and products of path B, computed with the PM3 method. Enthalpy of reaction (DE_{rn}) and activation energy(Ea) as depicted in Fig.(6)

Compounds	E_{total}	$\Delta E_{rn}1$	$\Delta E_{rn}2$	ΔE_{rn}(total)[b]	$Ea1$	$Ea2$
1	-60513.4					
a-1	-6869.8			-64.6		
a-2	-15769.8			-70.2		
a-3	-20666.7			-71.6		
a-4	-19955.7			-83.5		
Ina-1	-67407.9	-32.2				
Ina-2	-76300.5	-37.3				
Ina-3	-81198.1	-37.9				
Ina-4	-80479.7	-44.1				
Pa-1	-59958.3		-28.2			
Pa-2	-68838.1		-15.4			
Pa-3	-73750.7		-30.4			
Pa-4	-73023.1		-31.0			
Pa-11	-59962.5		-4.2[a]			
Pa-21	-68855.6		-17.5[a]			
Pa-31	-73754.0		-3.3[a]			
Pa-41	-73041.5		-8.4[a]			
N_2	-7477.8					
TSBa-1	-67351.0				32.2	
TSBa-2	-76245.9				37.3	
TSBa-3	-81142.2				37.9	
TSBa-4	-80425.0				44.1	
TSBa-11	-67372.4					35.5
TSBa-21	-76266.0					34.5
TSBa-31	-81158.4					39.7
TSBa-41	-80443.6					36.4

[a] DE_{rn}**3 (see Fig. 6).** [b] DE_{rn}**(total) =** DE_{rn}**1 +** DE_{rn}**2 +** DE_{rn}**3**

Table (6)

Calculated total energy in kcal mol^{-1}of reactants, transition states and products of path B, computed with the single point calculations on the HF/3-21G //AM1. Enthalpy of reaction(DE_{rn})and activation energy(Ea) as depicted in Fig. (6).

Compounds	E_{total}	$\Delta E_{rn}1$	$\Delta E_{rn}2$	ΔE_{rn}(total)[b]	*Ea*1	*Ea*2
1	-466604.5					
a-1	-48694.1			-103.0		
a-2	-120301.2			-107.6		
a-3	-146126.4			-111.8		
a-4	-145405.7			-96.4		
Ina-1	-515330.9	-32.3				
Ina-2	-586939.8	-34.1				
Ina-3	-612763.5	-32.6				
Ina-4	-612040.1	-30.0				
Pa-1	-447409.8		-37.8			
Pa-2	-519010.9		-30.0			
Pa-3	-544843.6		-39.0			
Pa-4	-544124.7		-43.5			
Pa-11	-447441.0		-40.2[a]			
Pa-21	-519045.4		-32.7[a]			
Pa-31	-5448473.8		-34.5[a]			
Pa-41	-544147.6		-22.9[a]			
N_2	-67958.9					
TSBa-1	-515274.2				24.4	
TSBa-2	-586886.4				19.3	
TSBa-3	-612707.3				23.6	
TSBa-4	-611983.9				26.3	
TSBa-11	-515311.1					19.8
TSBa-21	-586922.3					17.5
TSBa-31	-612739.9					23.6
TSBa-41	-612022.0					18.1

$DE_{rn}3$ (see Fig. 6). [b]*DE_{rn}(total) =$DE_{rn}1$ + $DE_{rn}2$ + $DE_{rn}3$*

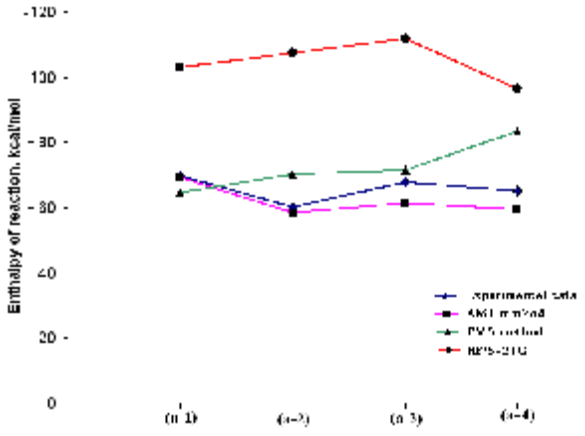

Fig. (11):Comparison of experimental data of enthalpies of reaction of the concerted Diels-Alder reactions of ethylene (a-1), cyclopentadiene (a-2), 1-hexene (a-3), cyclohexene (a-4) and dimethyl 1,2,4,5-tetrazine-3,6-dicarboxilate (1) with different levels of quantum calculations.

Conclusions

The present paper reports theoretical study on the inverse-demand synchronous concerted Diels-Alder reactions between dimethyl 1,2,4,5-tetrazine-3,6-dicarboxylate as diene and a variety of dienophiles (ethylene, cyclopentadiene, 1-hexene, cyclohexene) at different levels of quantum calculations (AM1, PM3 and ab initio (HF/3-21G)). The calculated activation energies and volumes at AM1 level showed that the cycloaddition systems followed a mechanism by formation an intermediate as a first step and proceed to eject N_2 molecule at second step and ended by 1, 2-hydrogen shift adduct. The present cycloaddition reactions show higher activation energies and higher exothermicities. The prediction of the reaction energies of modeling of the present cycloaddition reactions by semiempirical AM1 method showed a good agreement with the experimental data comparing with PM3 and HF/3-21G. Whereas, the prediction of activation

energies by (AM1, PM3 and ab initio (HF/3-21G)) showed overestimated values comparing with experimental data. However, the present study exposes the limitations of the semiempirical methodologies in modeling the Diels-Alder reactions. In contrast, the HF method overestimates the activation and reaction energies.

References

[1] a) J. P. Dell, *J. Chem. Soc., Perkin Trans.1* 1998, 3873; S.M. Weinreb, in: B.M. Trost, I. Fleming, L.A. Paquette(Eds.), Comprehensive Organic Synthesis, vol. 5, PergamonPress, Oxford, 1991; b) L. Stella, H. Abraham, J. Feneu-Dupont, B. Tinant, J.P.Declercq, Tetrahedron Lett. 31, 2063, 1990; c) A.R. Kadritzky, M.F. Gordeev, J. Org. Chem. 58, 4049, 1993; d) H. Mayr, A.R.Ofial, J. Sauer, B. Schmied, Eur. J. Org. Chem., 2013, 2000.

[2] a) J. Hamer, Ed. *1,4-Cycloaddition Reactions;* Academic Press: New York, 1967;Wasserman, A. *Diels-Alder Reactions:* Elsevier: New York, 1965; b) G. Brieger, J. N. Bennett, *Chem. Rev.*, 80, 63, 1980.

[3] a) M.A. McCarrick, Y.D. Wu, K.N. Houk, *J. Am. Chem. Soc.*, 114, 1499, 1992; b) M.A. McCarrick, Y.D. Wu, K.N. Houk, *J. Org. Chem.*, 58, 3330, 1993; c) L.R. Domingo, *J. Org. Chem.*, 66, 3211, 2001.

[4] a) C. Hedberg, P. Pinho, P. Roth, P.G. Andersson, *J. Org. Chem.*, 65 (2000) 2810; b) L.R. Domingo, M. Oliva, J. Andres, *J. Mol. Struct.(Theochem)*, 66, 6151, 2001; c) L.R. Domingo, M. Oliva, J. Andres, *J. Org. Chem.*, 66, 6151, 2001.

[5] a) R. Vijaya, G. Narahari Sartry, *J. Mol. Stru. (Theochem*), 618, 201, 2002 ; b) W. T. Borden, R. J. Loncharich and K. N. Houk, *Ann. Rev. Phys.Chem.*, 39, 213, 1988; c) K. N. Houk, Y. Li and J. D. Evanseck, *Angew Chem., Int. Ed. Engl.*, 31, 682, 1992; d) V. Branchadell, J. Orti, R. M. Ortuno, A. Oliva, J. Font, J. Bertran and J. J. Dannenberg, *J. Org. Chem.*, 56, 2190, 1991; e) V. Branchadell, M. Sodupe, R. M. Ortuno, A. Oliva, D. Gomez-Pardo, A. Guingant and J. d'Angelo, *J. Org. Chem.*, 56, 4135, 1991.

[6] a) D. L Boger,.*Chem. Rev.*, 86, 781, 1986; b) D. L Boger, S. M. Weinreb, *Hetero Diels-Alder Methodology in Organic Synthesis*; Academic: San Diego, 1987.

[7] a) D.L Boger, C. W. Boyce, M. A. Labroli, C. A. Sehon, Q. Jin, *J. Am. Chem. Soc.*, 121, 54, 1999; b) D. L. Boger, D. R. Soenen, C. W. Boyce, M. P. Hedrick, Q. Jin, *J. Org. Chem.*, 65, 2479, 2000; c) Boger, D. L., Hong, J., *J. Am. Chem Soc.*, 123, 851, 52001.

[8] R. A. Carbon, R. V. Lindsey Jr., *J. Am. Chem. Soc.*, 81, 4342, 1959.

[9] J.J.P. Stewart, in: K.B. Lipkowitz, D.B.V. Boyd (Eds.), *Reviews in computational Chemistry*, vol. 1, Wiley-VCH, New York, 1990.

[10] M. J. S. Dewar, E. G. Zoebisch, E. F. Healy, J. J. P. Stewart, *J. Am. Chem. Soc*., 107, 902, 1985.

[11] a) Stewart, J. J. P. *J. Comput. Chem.*, 10, 209, 1989; b) J. S. Binkley, J.A. Pople, W.J. Hehre, *J. Chem. Soc*.,102, 939,1980.

[12] N. Bodor, Z. Gabanyi, C. Wong, *J. Am. Chem. Soc.*,111, 3783, 1989.

[13] A. Gavezotti, *J. Am. Chem. Soc.*, 10, 5220, 1983.

[14] A. Bondi, *J. Phys. Chem.*, 68, 441, 1964.

[15] K. N. Houk, Y. Li, J. D. Evenseck, *Angew. Chem. Int. Ed. Engl.*, 31, 682, 1992.

[16] V. Branchadell, J. Orti, R. M. Ortuno, A. Oliva, J. Font, J. Bertran and J. J. Dannenberg, *J. Org . Chem.*, 56, 2190, 1991.

[17] V.D. Kiselev, E. A. Kashaeva , G.G. Iskhakova , M. S. Shihab and A. I. Konovalov, *Tetrahedron*, 55, 12201, 1999.

[18] J. D. Cox, G. Pilcher, *Thermochemistry of organic and organometallic compounds*, Academic press, London-N. Y., 643, 1970.

[19] R. Vijaya . T. C. Dinadayalane, G. Narahari Sartry, *J. Mole. Stru. (Theochem)*, 589-590, 291, 2002.